Spectral Shadowing Compensation in Double-pulse FBG-assisted φ-OTDR

F. Sandah[1,2], **M. Dossou**[1], **and M. Wuilpart**[2]

[1]PHORAN, EPAC, University of Abomey-Calavi, Calavi, Benin
[2]Electromagnetism and Telecommunications Unit, Faculty of Engineering
University of Mons, Mons, Belgium

2022 Photonics & Electromagnetics Research Symposium (PIERS) | 978-1-6654-6023-1/22/$31.00 ©2022 IEEE | DOI: 10.1109/PIERS55526.2022.9792714

Abstract— In this paper, a method to suppress the spectral shadowing effect in the frame of a double-pulse FBG-assisted phase-OTDR is proposed and experimentally demonstrated. The approach is based on the introduction of a small extra delay between the two pulses.

1. INTRODUCTION

Distributed optical fiber sensors (DOFS) have received important attention because of their significant advantages in many application fields such as crack detection [1], electrical discharge location [2], geophysical seismic data acquisition for earthquake identification and location [3, 4] and groundwater level monitoring [4]. Another significant application is structural health monitoring (SHM), which enables the monitoring in real-time of transportation infrastructures such as railroads [5], dams, tunnels, highways, bridges, and pipelines. SHM allows to detect defects on those infrastructures in order to prevent collapses or any other undesirable events [6]. DOFS aim to perform the distributed measurement of physical parameters such as temperature, pressure and vibration [1–7]. Some of DOFS are made with reflectometers sensitive to the phase of the Rayleigh backscattered signal or (phase-optical time domain reflectometer, φ-OTDR). φ-OTDR enables distributed vibration sensing by analyzing the interference properties of the backscattered signal when an optical pulse is launched in the sensing fiber. As the Rayleigh backscattered light power is quite weak (a few tens of dB below the pulse peak power), identical fiber bragg grating (FBG) arrays can be used to increase the signal to noise ratio [7]. In that context single-pulse and double-pulse configurations have been proposed to interrogate a cascade of FBG and to measure the interference resulting from two successive FBGs. Compared to the single-pulse approach, the double-pulse configuration enables the reduction of the Rayleigh backscattered noise [8]. However, using identical FBGs generates undesirable effects such as spectral shadowing. Spectral shadowing is a distortion of the signal reflected by an FBG and measured by the φ-OTDR that is induced by all the upstream FBGs [9]. As a consequence if a vibration is applied on a given FBG of the sensing fiber, its frequency content will be included in all the interference signals resulting from two successive FBGs located downstream. Ghost frequencies will therefore be recorded by the sensor, resulting to an erroneous vibration diagnosis. Spectral shadowing compensation has already been demonstrated by our team in the case of single-pulse FBG-assisted φ-OTDR [9]. In this paper, a spectral shadowing compensation technique is proposed in the context of a double-pulse FBG-assisted φ-OTDR. In Section 2, the sensor principle is presented as well as the compensation method. Section 3 is dedicated to the experimental validation of the proposed approach.

2. PRINCIPLE OF DOUBLE-PULSE FBG-ASSISTED φ-OTDR

The FBG-assisted φ-OTDR based on double-pulse interrogation was proposed in [8]. Compared to the single-pulse approach [9], the double-pulse configuration enables using shorter pulse duration, resulting to a smaller Rayleigh-induced noise level. The double-pulse approach allows measuring the interference of the signals reflected by two successive FBGs if the delay between the pulses corresponds in the spatial domain to twice the distance between two successive FBGs (denoted by L_{FBG}) and if the coherence length of the laser source is much larger than $2L_{\mathrm{FBG}}$. The interference signal is sensitive to any external vibration applied between the two FBGs since it will locally modify the propagation constant. Figure 1 shows a section of the sensing fiber with two identical successive FBGs (FBG_A and FBG_B). Let us consider that this configuration is interrogated by a double pulse. The first pulse is partially reflected by FBG_A, and the φ-OTDR detects the P_A power. No signal is then detected until the first pulse is partially reflected by FBG_B. The reflected signal from FBG_B returns and passes through the FBG_A a second time and overlaps with the signal corresponding to the second pulse reflected by FBG_A. The resulting interference signal is denoted by P_{AB}. This interference appears since the distance between the two pulses is equal to twice the distance between the two FBGs (round trip time of the first pulse between the two FBGs). A third peak appear in the φ-OTDR due to the second pulse reflected by FBG_B.

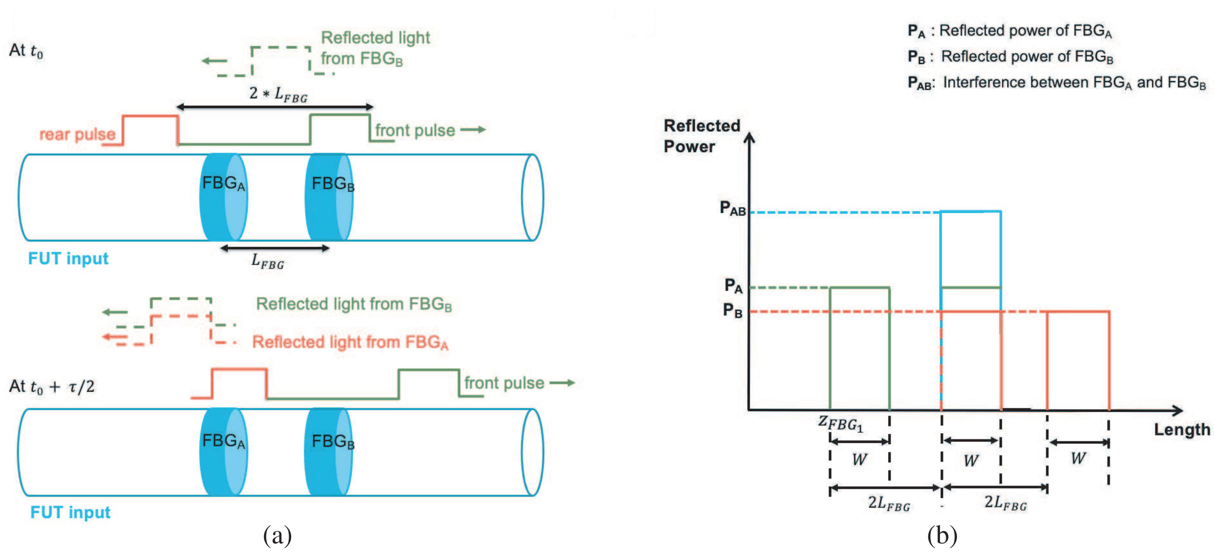

Figure 1: Double-pulse principle.

3. EXPERIMENT

The experimental setup is presented in Figure 2. It is composed of the source, the FUT (Fiber Under Test) and the receiver. The light source consists of an ultra-narrow linewidth laser (NLL) emitting a highly coherent and continuous light with a linewidth of 0.1 kHz and a wavelength of 1552.5 nm. A pulse function generator (PG) enables to generate a pulse electrical signal sent to an acousto-optic modulator (AOM) which modulates the continuous lightwave to obtain a double-pulse configuration so that the pulse duration is equal to 60 ns and the delay is set to 80 ns with a repetition rate of 20 kHz. The pairs of pulses are amplified by an erbium doped fiber amplifier (EDFA) and filtered by a bandpass filter (BPF, bandwidth of 1 nm) and finally launched into the FUT through the first port of an optical circulator. The backscattered/reflected light is guided to the receiver through port 3 of the circulator. The receiver is composed of an optical amplifier, a photodetector (PD) with a transimpedance gain amplifier and a data acquisition card with 1 GS/s sampling rate.

To study the effect of spectral shadowing crosstalk, four low reflectivity (0.04%) FBGs have been inscribed in the FUT. The four FBGs share globally the same characteristics, having a length

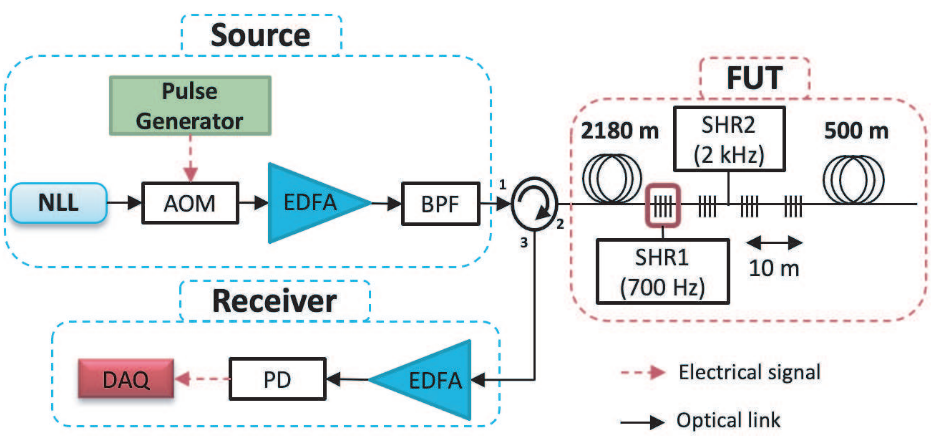

Figure 2: Experimental setup.

of 4 mm, a center wavelength of 1552.5 nm and a 3 dB bandwidth of 0.2 nm. The grating pitch is equal to 536.42 nm. Two successive FBGs are separated by 10 m ($L_{\mathrm{FBG}} = 10$ m). The array is preceded by a lead-in fiber spool of 2.18 km and terminated by a fiber spool of 0.5 km length. The first FBG (FBG_1) is attached to a shaker (SHR1). The 10 m distance between the second and the third FBGs is attached to an plastic tube connected at its midpoint to shaker SHR2. Unlike the first FBG, the others are static. The plastic tube has its ends clamped. SHR1 is driven by a sinusoidal signal at 700 Hz with a 1 g acceleration and SHR2 is driven by a sinusoidal signal of 2 kHz with a 0.1 g acceleration.

4. PRINCIPLE OF THE SPECTRAL SHADOWING COMPENSATION METHOD

The FBG-assisted φ-OTDR configuration presented so far is subject to spectral shadowing. As described in Section 1, spectral shadowing occurs when a concatenation of gratings sharing the same spectral characteristics are addressed simultaneously. Distortion occurs in the downstream FBGs spectra due to light passing twice through an upstream FBG. The main idea of the proposed compensation method is to interrogate the cascade of FBGs with a double-pulse signal for which an extra delay between the two pulses has been generated. This extra delay is obtained by reducing the delay between the two pulses to $2kL_{\mathrm{FBG}}$ where k is the reduction coefficient ($k \in [1-\frac{W}{2L_{\mathrm{FBG}}}, 1]$ when W is the pulse width). This additional delay allows to obtain extra data on the phase-OTDR trace: the signals reflected independently by each FBG can also be measured (not only their interference). As explained later, this extra information can be used to remove the spectral shadowing. Let us note that the signals reflected by two successive FBGs still overlap over a distance of $W - 2(1-k)L_{\mathrm{FBG}}$ so that the interference signal is still accessible.

The compensation principle is shown in Figure 3. Let us first suppose that $k = 1$ so that the distance between the front and rear pulses is equal to $2L_{\mathrm{FBG}}$. When the two pulses propagate down the fiber, the signals reflected by two adjacent FBGs overlap and the interference signal is detected at the OTDR. In the specific case of $k = 1$, the overlap is perfect and the φ-OTDR trace is as shown in Figure 3(c) where the interference peaks appear (P_{AB} for instance). Reducing the distance between the pulses by a factor k, the φ-OTDR signal will show extra power levels as P_A and P_B resulting from the power reflected independently from FBG_A and FBG_B, respectively, over a distance of $2(1-k)L_{FBG}$ (see Figure 3(d)).

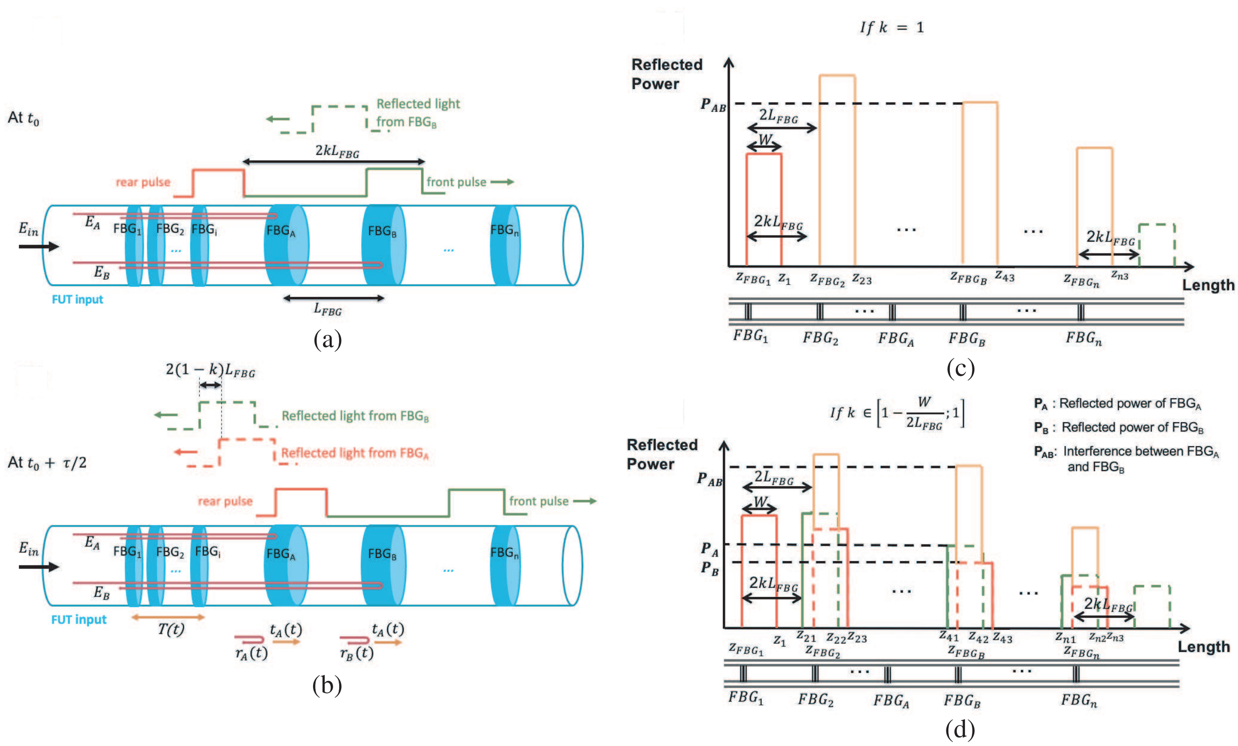

Figure 3: (a)–(b) Principle of double-pulse within sensing fiber embedded of n identical FBGs; typical φ-OTDR trace versus position over the time for (c) $k = 1$ and (d) $k \in [1 - \frac{W}{2L_{\mathrm{FBG}}}, 1]$.

Each FBG is characterised by the magnitude and the phase of its reflection and transmission complex coefficients r and t. They depend on parameters such as effective refractive index, index modulation depth, periodicity, visibility and grating length [10]. Considering a complex electric field E_{in} at the FBG array input, a complex reflection coefficient r_A (r_B) for FBG_A (FBG_B) and complex transmission coefficient t_A for FBG_A, the electric fields E_A and E_B reflected respectively by FBG_A and FBG_B and observed at the sensing fiber input are given by [9]:

$$E_A = E_{in}T^2(t)r_A(t) \tag{1}$$

$$E_B = E_{in}T^2(t)t_A^2(t)r_B(t)e^{j\Delta\varphi(t)} \tag{2}$$

with $T(t)$ the product of the complex transmission coefficients of all $FBGs$ preceding FBG_A and $\Delta\varphi(t)$ twice phase difference between FBG_A and FBG_B. $\Delta\varphi(t)$ contains information about external effect (here a vibration) applied between FBG_A and FBG_B. Based on Eqs. (1) and (2), the reflected powers defined in the previous paragraph yield:

$$P_A = E_AE_A^* = |E_{in}|^2|T(t)|^4|r_A(t)|^2 \tag{3}$$

$$P_B = E_BE_B^* = |E_{in}|^2|T(t)|^4|t_A(t)|^4|r_B(t)|^2 \tag{4}$$

$$\begin{aligned} P_{AB} &= E_{AB}E_{AB}^* = |E_{in}|^2|T(t)|^4|r_A(t)|^2 + |E_{in}|^2|T(t)|^4|t_A(t)|^4|r_B(t)|^2 \\ &\quad +2|E_{in}|^2|T(t)|^4|t_A(t)|^2|r_A(t)||r_B(t)|\cos(\Delta\varphi(t)+\theta(t)) \end{aligned} \tag{5}$$

where $\theta(t) = \arg[r_B(t)/r_A(t)]$. As $T(t)$ is the product of the complex transmission coefficients of all FBGs preceding FBG_A, it is responsible for the generation of spectral shadowing in the interference power P_{AB} if one or several of the preceding FBGs is subject to an external vibration. By using Eqs. (3), (4) and (5), it can be shown that the spectral shadowing can be compensated by a proper arrangement of P_A, P_B and P_{AB} [9]:

$$\frac{P_{AB}(t) - P_A(t) - P_B(t)}{2\left(\sqrt{P_A(t)}\sqrt{P_B(t)}\right)} = \cos(\Delta\varphi(t)+\theta(t)) \tag{6}$$

The result of this mathematical operation does not depend on $T(t)$. It therefore allows to suppress the spectral shadowing. In the next section, the proposed approach is experimentally validated.

Figure 4 shows the supperposition of φ-OTDR traces detected after interrogating the FUT many times with a frequency of 20 kHz. Since the delay between the front and the rear pulses is set to 80 ns and $L_{\text{FBG}} = 10\,m$, the reduction coefficient k is equal to 0.8. The φ-OTDR detects five different peaks: the peak related to the power reflected by FBG_1, three interference peaks corresponding to the three successive pairs (FBG_1 and FBG_2, FBG_2 and FBG_3, FBG_3 and FBG_4) and a peak related to the power reflected by FBG_4. The reducing delay between the pulses allows to obtain three different power levels in each FBG pair peak as shown in Figure 4 for the FBG_2-FBG_3 pair: P_A, P_B and P_{AB} can be identified. Therefore, the application of the compensation formula (6) can be applied to suppress the spectral shadowing.

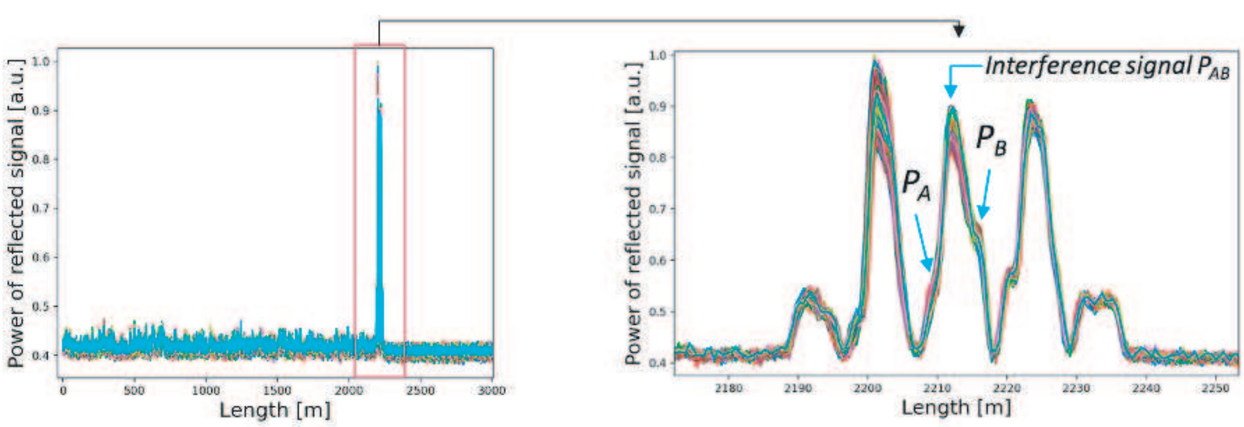

Figure 4: Experimental φ-OTDR trace: detected reflected signal power versus position over time (zoom 2180–2250 m).

Figure 5(a) shows the reflected power P_{AB} as a function of time and Figure 5(b) its fast Fourier transform (FFT). It corresponds to the signal detected at 2212 m, i.e., the position of the interference peak related to FBG_2 and FBG_3 in between which the 2 kHz vibration is applied. The frequency of 2 kHz was easily detected. It also clearly appears that at the same position, an unwanted frequency component at 700 Hz is observed. This is induced by the vibration applied on the first FBG at 2190 m through spectral shadowing. After applying the compensation formula (6), the spectral shadowing is suppressed. Figure 5(c) shows the compensated power as a function of time and Figure 5(d) its FFT. Clearly, the result shows that the proposed approach enables to remove the spectral shadowing.

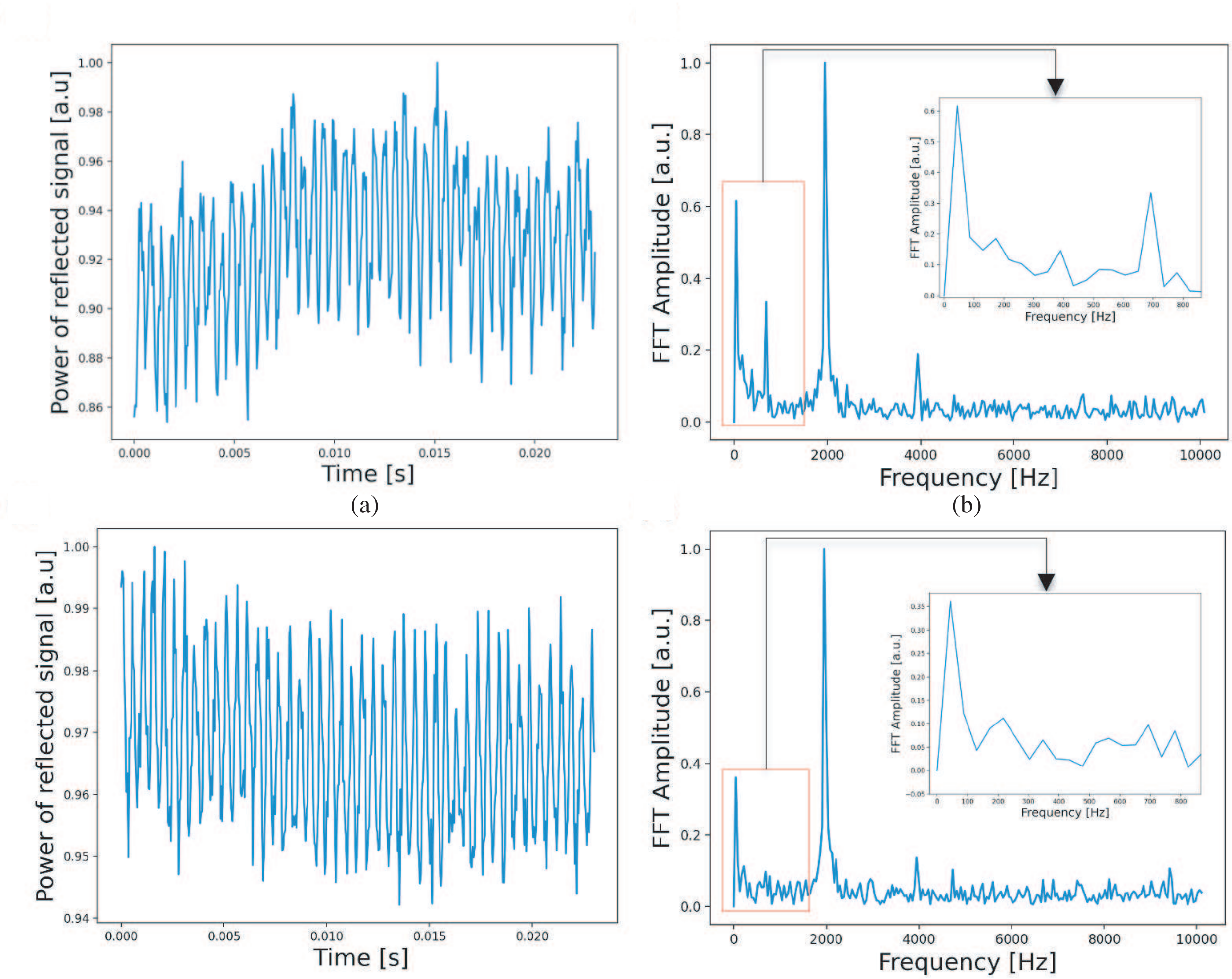

Figure 5: (a) P_{AB} as a function of time and (b) its FFT (inset: zoom 0–800 Hz) around 2212 m; (c) compensated power as a function of time and (d) its FFT (inset: zoom 0–800 Hz) around 2212 m.

5. CONCLUSION

In this paper, a spectral shadowing compensation technique is proposed. The main idea is to interrogate the cascade of identical weak FBGs with a double pulse signal for which an extra delay between the two pulses has been generated. This additional delay allows extra data on the phase-OTDR trace: the signals reflected independently by each FBG can also be measured. This extra information can be used to remove the spectral shadowing. The compensation method was theoretically explained and tested on a cascade of four identical FBGs separated by 10 m.

REFERENCES

1. Chapeleau, X., J. Blanc, P. Hornych, J. L. Gautier, and J. Carroget, "Assessment of cracks detection in pavement by a distributed fiber optic sensing technology," *Journal of Civil Structural*

Health Monitoring, Vol. 7, No. 4, 459–470, 2017.

2. Ma, G. M., C. Shi, W. Q. Qin, Y. B. Li, H. Y. Zhou, and C. R. Li, "A non-intrusive electrical discharge localization method for gas insulated line based on phase-sensitive OTDR and Michelson interferometer," *IEEE Transactions on Power Delivery*, Vol. 34, No. 4, 1324–1331, 2019.
3. Jousset, P., T. Reinsch, T. Ryberg, H. Blanck, A. Clarke, R. Aghayev, G. P. Hersir, J. Henninges, M. Weber, and C. M. Krawczyk, "Dynamic strain determination using fibre-optic cables allows imaging of seismological and structural features," *Nature Communications*, Vol. 9, No. 1, 1–11, 2018.
4. Ajo-Franklin, J. B., S. Dou, N. J. Lindsey, I. Monga, C. Tracy, M. Robertson, V. R. Tribaldos, C. Ulrich, B. Freifeld, T. Daley, and X. Li, "Distributed acoustic sensing using dark fiber for near-surface characterization and broadband seismic event detection," *Scientific Reports*, Vol. 9, No. 1, 1–14, 2019.
5. Wang, Z., B. Lu, H. Zheng, Q. Ye, Z. Pan, H. Cai, R. Qu, Z. Fang, and H. Zhao, "Novel railway-subgrade vibration monitoring technology using phase-sensitive OTDR," *25th Optical Fiber Sensors Conference (OFS)*, 1–4, April 2017.
6. Tennyson, R. C., A. A. Mufti, S. Rizkalla, G. Tadros, and B. Benmokrane, "Structural health monitoring of innovative bridges in Canada with fiber optic sensors," *Smart Materials and Structures*, Vol. 10, No. 3, 560, 2001.
7. Yüksel, K., J. Jason, E. B. Kocal, M. L. A. Sainz, and M. Wuilpart, "An overview of the recent advances in FBG-assisted phase-sensitive OTDR technique and its applications," *22nd International Conference on Transparent Optical Networks (ICTON)*, 1–7, IEEE, July 2020.
8. Liu, T., F. Wang, L. Zhou, X. Zhang, and L. Zhang, "Phase sensitive distributed vibration sensing using double-pulse for ultra-weak FBG array," *Conference on Lasers and Electro-Optics/Pacific Rim Optical Society of America*, s0978, July 2017.
9. De Miguel Soto, V., J. Jason, D. Kurtoğlu, M. Lopez-Amo, and M. Wuilpart, "Spectral shadowing suppression technique in phase-OTDR sensing based on weak fiber Bragg grating array," *Optics Letters*, Vol. 44, No. 3, 526–529, 2019.
10. Erdogan, T., "Fiber grating spectra," *Journal of Lightwave Technology*, Vol. 15, No. 8, 1277–1294, August 1997.